Chapter 6
Characterisation of Micro-Sized and Nano-Sized Tungsten Oxide-Epoxy Composites for Radiation Shielding of Diagnostic X-Rays

Abstract Characteristics of X-ray transmissions were investigated for epoxy composites filled with 2–10 vol.% WO_3 loadings using synchrotron X-ray Absorption Spectroscopy (XAS) at 10–40 keV. The results obtained were used to determine the equivalent X-ray energies for the operating X-ray tube voltages of mammography and radiology machines. The results confirmed the superior attenuation ability of nano-sized WO_3-epoxy composites in the energy range of 10–25 keV when compared to their micro-sized counterparts. However, at higher synchrotron radiation energies (i.e., 30–40 keV), the X-ray transmission characteristics were similar with no apparent size effect for both nano-sized and micro-sized WO_3-epoxy composites. The equivalent X-ray energies for the operating X-ray tube voltages of the mammography unit (25–49 kV) were in the range of 15–25 keV. Similarly, for a radiology unit operating at 40–60 kV, the equivalent energy range was 25–40 keV, and for operating voltages greater than 60 kV (i.e., 70–100 kV), the equivalent energy was in excess of 40 keV. The mechanical properties of epoxy composites increased initially with an increase in the filler loading but a further increase in the WO_3 loading resulted in deterioration of flexural strength, modulus and hardness.

6.1 Introduction

Hitherto, numerous analytical methods have been developed to investigate the effect of the particle size of a material on the X-ray attenuation for various incoming X-ray energies including scattered gamma-rays and X-rays [1–11]. It is widely believed that nano-sized particles are able to disperse more uniformly within the matrix with fewer agglomerations when compared to micro-sized particles, thus improving the X-ray attenuation ability of the material [6, 12, 13]. For instance, Hołyńska [4] found that the intensity of scattered radiations increased with increases in the grain size of a material. This size effect has been observed in a sand matrix and for samples containing heavy elements such as iron or barium [4].

Filler-reinforced polymers have gained increasing attention from X-ray technologists in radiation shielding since polymers have great potential in many important applications by virtue of their unique properties, such as low density, the ability to

I. M. Low and N. Z. Noor Azman, *Polymer Composites and Nanocomposites for X-Rays Shielding*, Composites Science and Technology,
https://doi.org/10.1007/978-981-13-9810-0_6

form intricate shapes, optical transparency, low manufacturing cost and toughness. One of the filler-reinforced polymers commonly used for radiation shielding is lead acrylic [14–16]. Moreover, some researchers have also tried to synthesise nano-sized filler-reinforced polymers for radiation shielding by virtue of the size effect in X-ray attenuation [2, 6, 17]. For instance, a recent study by Botelho et al. [13] revealed that the attenuation for X-ray beams generated from low tube voltages (i.e., 26–30 kV) in nanostructured copper oxide (CuO) was better than microstructured CuO. However, no significant difference in attenuation was observed for X-rays generated from higher tube voltages (i.e., 60–102 kV). A similar conclusion on this size effect in X-ray attenuation was made by Künzel and Okuno [18] for a nanostructured CuO-polymer system.

In a recent work on WO_3-filled epoxy composites [19], we investigated the effect of nano-sized and micro-sized WO_3 filler-epoxy composites on X-ray attenuation in the X-ray tube voltage range of 22–127 kV generated by a mammography unit and a general radiography unit. The equivalent X-ray energies for the various X-ray tube voltages used were in the range of 17.5–60 keV, which conformed to our expectation since the equivalent X-ray energies for a mammography unit were 17.5, 19.6, 20.2 and 22.7 keV which are the characteristic energies of molybdenum and rhodium; while the equivalent X-ray energy for a radiology unit is about one-third of the X-ray tube voltage used. The results showed that nano sized WO_3 was more effective than micro-sized WO_3 in X-ray attenuation only in the low X-ray tube voltage range of 22–35 kV but this size effect was not apparent at the higher X-ray operating tube voltage range of 40–120 kV [19]. Hence, the aim of this work was to verify our previous work on X-ray transmission in WO_3-filled epoxy composites by using synchrotron radiations as the X-ray source for the characteristic (monochromatic) X-ray energy range of 10–40 keV. The results obtained were compared with those of previous work [19] to determine the equivalent energy range of the previous machines used (a mammography unit and a radiology unit).

6.2 Results and Discussion

6.2.1 Characteristics of X-Ray Transmissions

Since the synchrotron radiations of the XAS beamline contain a large range of energies (i.e., 10–40 keV), the thickness of the samples was set at 2 mm to ensure that the detector was able to obtain a meaningful X-ray transmission reading for the lower energy range without being totally absorbed by the samples. As shown in Fig. 6.1, there was an obvious difference in X-ray transmissions between the micro-sized WO_3-epoxy and nano-sized WO_3-epoxy composites of the same WO_3 vol.% at the energy range of 10–20 keV. With a further increase of synchrotron energy to greater than 20 keV, there was no difference in X-ray transmissions between these two composites, thus indicating the absence of size effect at play. The results show that for

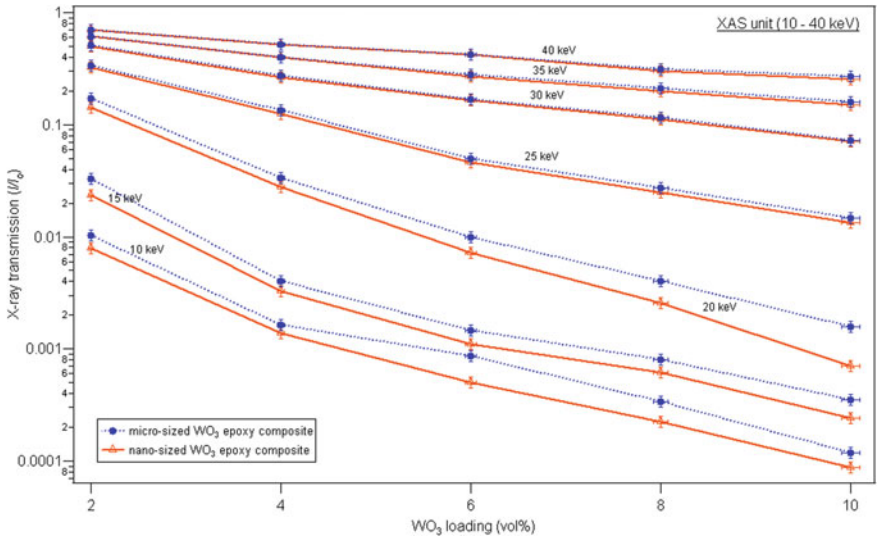

Fig. 6.1 Comparisons of X-ray transmission comparison in nano-sized and micro-sized WO_3-epoxy composites for synchrotron radiation generated by the XAS unit for energy of 10–40 keV [20]

all the WO_3 loadings in an epoxy matrix, the ratio of the X-ray transmission of the micro-sized WO_3-epoxy composite $(I/I_o)_m$ relative to the nano-sized WO_3-epoxy composite $(I/I_o)_n$, $(I/I_o)_m/(I/I_o)_n$ remained at ~1.0 for the synchrotron energy range of 25–40 keV. On the other hand, the ratio $(I/I_o)_m/(I/I_o)_n$ was 1.15–2.3 for all WO_3 loadings (see Fig. 6.2). The values determined for $(I/I_o)_m/(I/I_o)_n$ at these energy ranges indicate that the nano-sized WO_3-epoxy samples absorbed more low energy X-rays than their micro-sized WO_3-epoxy counterparts.

Further investigations were conducted to verify our previous results [19] obtained from a mammography unit and a radiography unit. In this investigation, all the same measurements from the previous work were repeated with samples of 2 mm in thickness. Since a mammography unit generates characteristic X-ray energies of molybdenum (17.5 and 19.6 keV) or rhodium (20.2 and 22.7 keV), it is much easier to compare with the XAS results (see Fig. 6.3). In the results presented in Fig. 6.3, it is clearly shown that the X-ray transmission results for the mammography unit sat between the results of 15–25 keV for the XAS beam energies. In contrast, for the radiography unit, the operated X-ray tube voltages generated a broad spectrum (polychromatic X-ray beam). Thus, the equivalent energies for the X-ray tube voltages of the radiography unit were estimated from the XAS results by superimposing their data together (see Fig. 6.4). As can be seen in Fig. 6.4, the X-ray transmissions of samples for X-ray tube voltages of 40–60 kV were sitting between 25 and 40 keV while the others were sitting above 40 keV. Hence, the X-ray tube voltages of 40–60 kV operated by the radiography unit produced the equivalent X-ray energies in

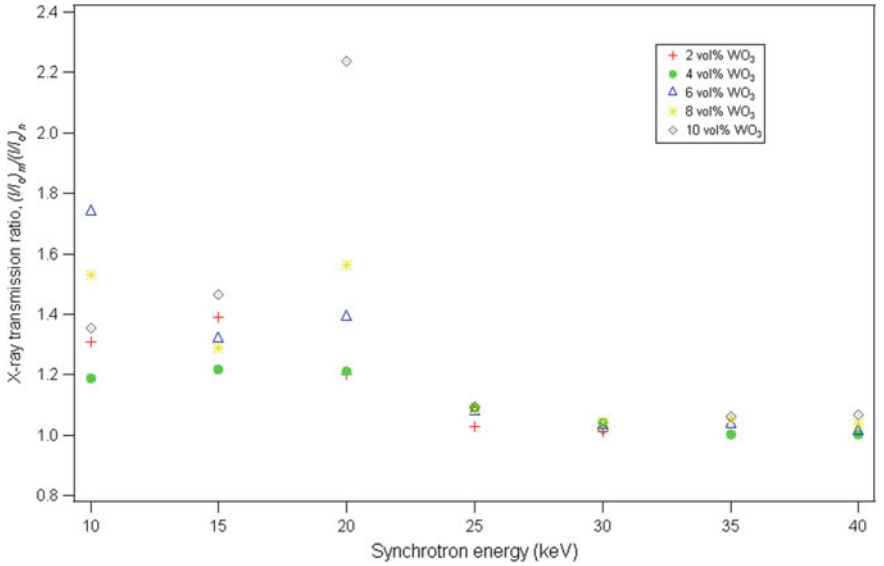

Fig. 6.2 The X-ray transmission ratio of micro-sized WO_3-epoxy composite $(I/I_o)_m$ to the X-ray transmission for nano-sized WO_3-epoxy composite $(I/I_o)_n$, $(I/I_o)_m/(I/I_o)_n$ for synchrotron energies (10–40 keV) [20]

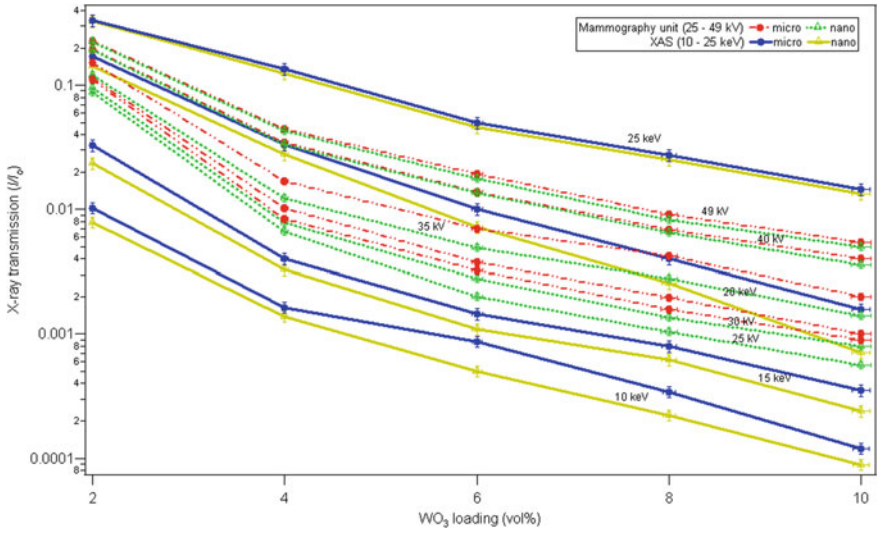

Fig. 6.3 Comparisons of X-ray transmission in nano-sized and micro-sized WO_3-epoxy composites for synchrotron radiation generated by the XAS unit for energies of 10–25 keV and mammography unit tube voltages of 25–49 kV [20]

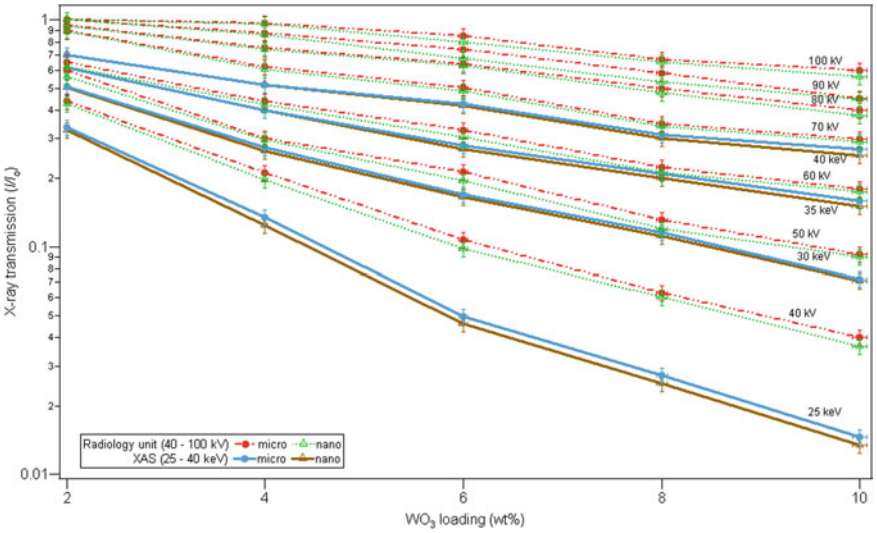

Fig. 6.4 Comparisons of X-ray transmission in nano-sized and micro-sized WO_3-epoxy composites for synchrotron radiation generated by the XAS unit for energies of 25–40 keV and radiography unit tube voltages of 40–100 kV [20]

the range of 25–40 keV while the X-ray tube voltages of ≥60 kV had an equivalent energy of ≥40 keV.

Figure 6.5 shows the comparison of X-ray transmissions for samples with different thicknesses. Samples of 7 mm thickness were used in our previous study [19], whereas 2 mm thick samples were used in this study. Figure 6.5a, b provide the results for the mammography unit only on samples with 4 and 6 vol.% loading of WO_3 respectively. As shown in these figures, the differences in the X-ray transmission between the micro-sized and nano-sized WO_3-epoxy became larger for thicker samples (7 mm). In contrast, Fig. 6.5c shows insignificant differences in X-ray transmission between nano-sized and micro-sized WO_3-epoxy composites for radiography tube voltages only for samples with a loading of 4 vol.% WO_3. This trend was also observed for all the other loadings (i.e., 2, 6, 8 and 10 vol.% WO_3). These findings are in good agreement with the work by Künzel and Okuno [18], which also showed that the grain size effect increased with the increase of the sample thickness at low energy X-ray beams (25 and 30 kV) but remained unchanged over the material thickness for higher energy X-ray beams (60 kV) [18].

In general, the photoelectric effect is the most likely interaction to occur within a matter at a lower photon (X-ray) energy range. In this interaction, a photon will transfer its entire energy to an electron in the material on which it impinges. The electron thereby acquires enough energies to free itself from the material to which it is bound and then may undergo single or multiple-scattering events with neighbouring atoms. In addition, there is also a slight fluctuation in the probability of emission of Auger electrons and fluorescent photons may form during this interaction. This

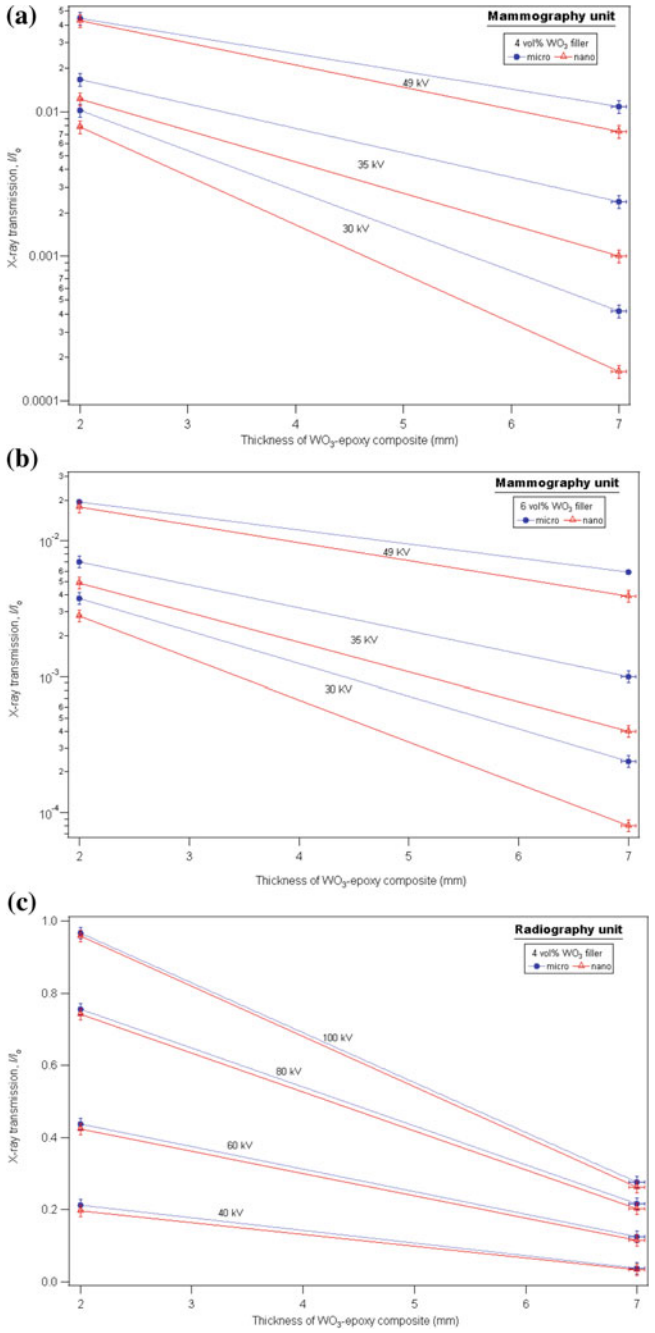

Fig. 6.5 X-ray transmission comparison for different thickness of the sample for **a** 4 vol.% of WO_3 filler epoxy composites for mammography unit tube voltages of 30, 35 and 49 kV; **b** 6 vol.% of WO_3 filler epoxy composites for mammography unit tube voltages of 30, 35 and 49 kV; and **c** 4 vol.% of WO_3 filler epoxy composites for radiography unit tube voltages of 40, 60, 80 and 100 kV [20]

phenomenon can contribute to the alteration of the mass attenuation coefficient of an element relative to the bulk material when considered over a small range of X-ray energies. The probability of photoelectric interaction is directly proportional to the cube of the atomic number of the absorbing material Z^3 and inversely proportional to the cube of the X-ray energy $(1/E)^3$.

Moreover, nano-sized WO_3-epoxy composites consist of a higher number of WO_3 particles/gram when compared to micro-sized WO_3-epoxy composites. Therefore, the distribution of the nano sized WO_3 in the resin should also be different from that presented by micro-sized WO_3, thus resulting in a more uniform dispersion in the resin. Therefore, the chances of an X-ray photon with lower energy to interact and be absorbed by WO_3 particles may be higher in nano-sized WO_3-epoxy composites than in micro-sized WO_3-epoxy composites. Figure 6.6 shows the back-scattered images of the same loading of WO_3 (4 vol.%) within nano-sized WO_3-epoxy and micro-sized WO_3-epoxy composites using the Zeiss Evo 40XVP scanning electron microscope. The WO_3 particles were seen to be more closely dispersed in the nano-sized WO_3-epoxy composite (Fig. 6.6a) as compared to its micro-sized counterpart (Fig. 6.6b). Thus, the probability for the lower energy photons to interact with the WO_3 particles and be absorbed is higher for the nano-sized WO_3-epoxy composite.

As the photon energy increases, the photon (X-ray) penetration through the absorbing material without interaction increases and hence, less photoelectric effect relative to the Compton affect occurs. Thus, the X-ray attenuation by the absorbing material decreased since the Compton interaction was weakly dependent on Z and E and this interaction only took place between the incident photon and one of the outer shell electrons of an atom in the absorbing material.

In order to discover the X-ray shielding ability of the composites, the results were compared to commercial lead (Pb) sheets (model RAS20 Calibrated Absorber Set) of four different thicknesses (i.e., 0.81, 1.63, 3.18 and 6.35 mm) (see Fig. 6.7) using a radiography unit of tube voltages 40–100 kV. The results show that although the lead sheets gave the lowest X-ray transmissions at each tube voltage when compared to

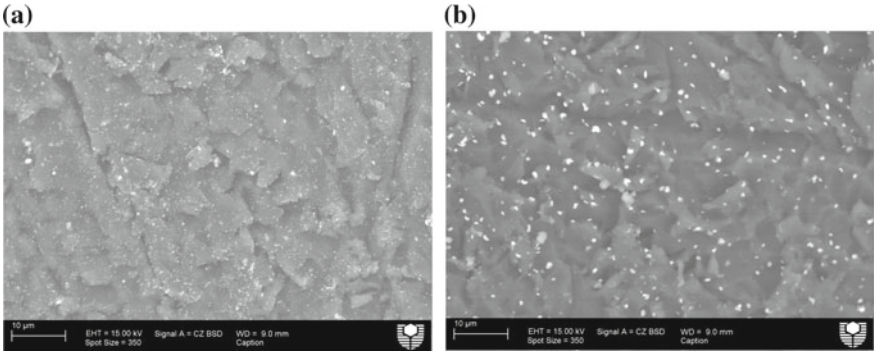

Fig. 6.6 SEM images for epoxy composites filled with **a** 4 vol.% nano-sized WO_3, and **b** 4 vol.% of micro-sized WO_3 [20]

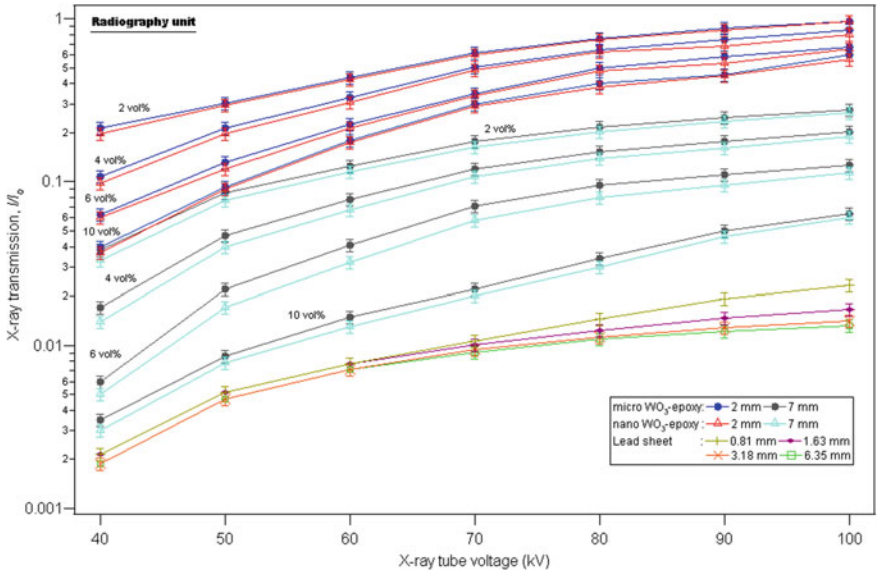

Fig. 6.7 X-ray transmission as a function of radiography unit X-ray tube voltage (40–100 kV) for all micro-sized and nano-sized WO_3-epoxy composites and commercial lead sheets [20]

all compositions of WO_3-epoxy composites, the latter with 10 vol.% of either micro-sized or nano-sized WO_3 can be a substitute for Pb in X-ray shielding by increasing the sample thickness to $\geq$7 mm. Hence, the usage of lead in X-ray shielding can be substituted by WO_3 whereby W is lighter and less toxic compared to Pb.

6.2.2 Crystallite Size

The reference for fitting the peaks was taken from the International Centre for Diffraction Data PDF-4+ 2009 database. The wavelength for all of these databases was chosen to be the same as the wavelength of the synchrotron radiation used. The diffraction peaks shown in Fig. 6.8 belong to monoclinic WO_3 (PDF file 00-043-1035). These results indicate that both the micro-sized WO_3 and the nano sized WO_3 were single-phase pure without impurities.

The diffraction patterns were plotted only in the 2θ range of 9–15° to clearly show the size difference of the peaks for each micro-sized and nano-sized WO_3. As shown in Fig. 6.8, the broad peaks belonged to nanometer-sized WO_3 crystallite whereas the well-defined crystalline peaks belonged to micrometer-sized WO_3. The crystallite size determined from the Scherrer equation for nano sized WO_3 was 51.5 nm. These nano-crystallites were significantly smaller than the particle sizes provided by Sigma-Aldrich, thus indicating that at least 2 crystallites were present in each WO_3 particle of 100 nm in size.

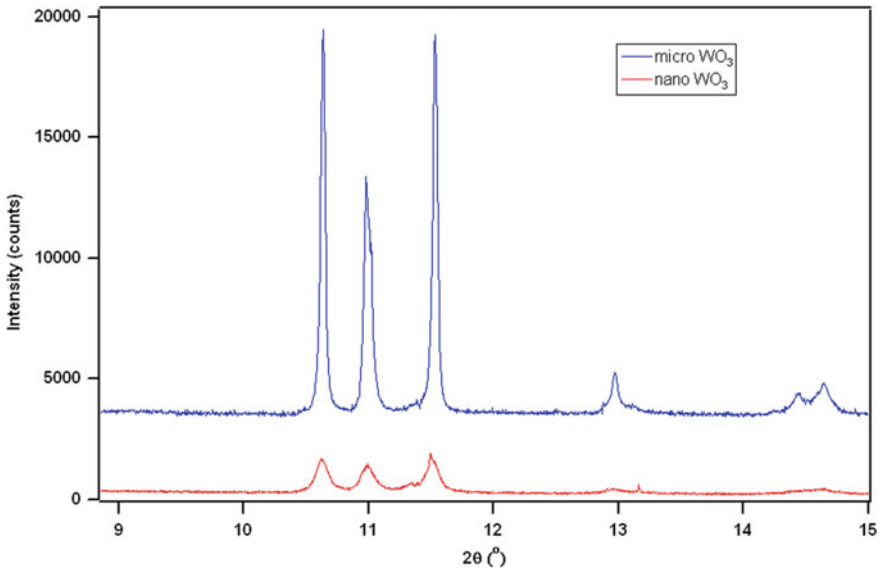

Fig. 6.8 Typical powder diffraction patterns for micro-sized and nano-sized WO_3 loading in epoxy composites [20]

6.2.3 Mechanical Properties

Figure 6.9 shows the effect of filler loading on the flexural strength, flexural modulus and Rockwell hardness of the epoxy composites. The flexural strength was found to decrease with increased WO_3 filler size while it had little or no effect on flexural modulus. Similar results were reported by Park [21] who observed an increase in flexural strength with decreased particle size in silica-reinforced epoxy composites. However, Moloney et al. [22] reported a negligible effect of particle size on flexural modulus in their epoxy composites filled with silica.

From Fig. 6.9a, the flexural strength of pure epoxy was 49.9 MPa but increased to a maximum value of 64 MPa for the composite containing 4 vol.% nano sized WO_3. However, a further increase in the filler loading beyond 4 vol.% resulted in a decrease in flexural strength whereby the composite containing 10 vol.% nano sized WO_3 exhibited the lowest flexural strength of 52.6 MPa. Similarly, for micro-sized WO_3-epoxy composites, the maximum flexural strength was obtained for a filler loading of 2 vol.%. A reduction in flexural strength was again observed when the filler loading was increased beyond 2 vol.% due to non-uniform dispersion of the filler within the matrix. The resultant agglomeration of the fillers acted as stress-concentrators which served to reduce the strength of the composites.

The flexural modulus of the composites increased with an increase in the filler loading for both the nano-sized and micro-sized WO_3 which may indicate that the stiffness of these composites obeyed the well-known rule-of-mixtures (Fig. 6.9b).

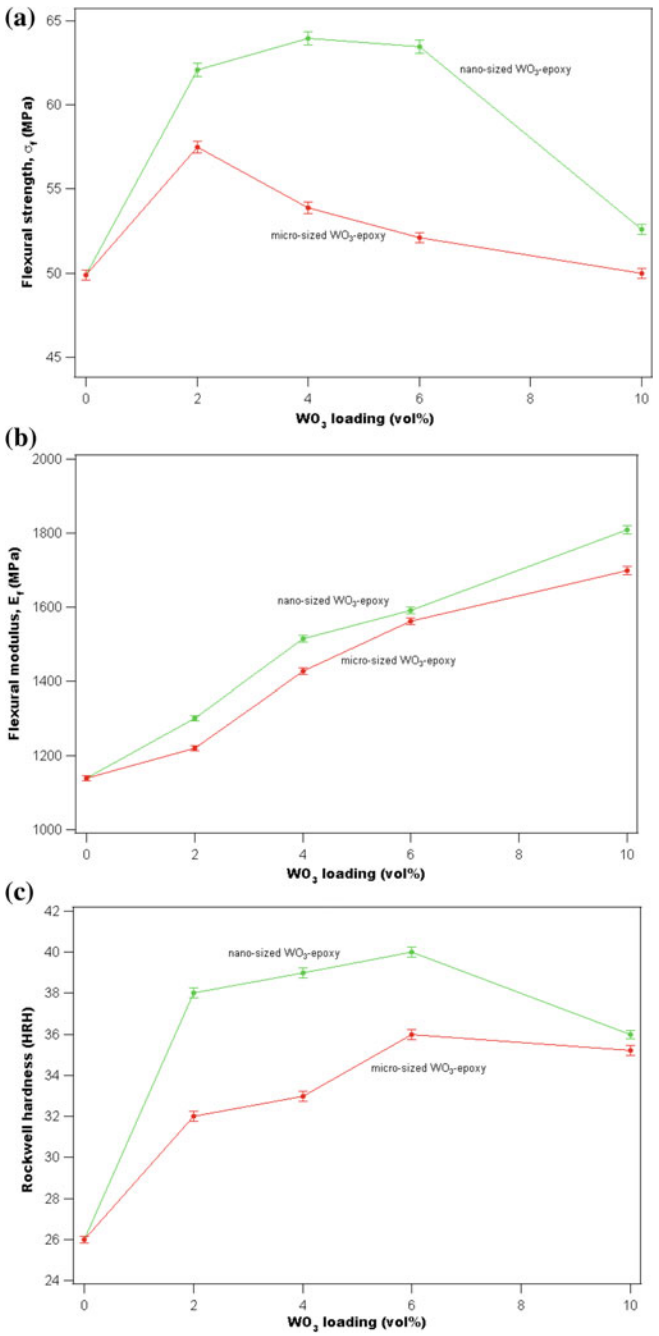

Fig. 6.9 Mechanical properties of epoxy composites showing: **a** flexural strength as a function of WO_3 filler loading; **b** flexural modulus as a function of WO_3 filler loading; and **c** Rockwell hardness as a function of WO_3 filler loading [20]

Finally, the hardness results presented in Fig. 6.9c indicate that an increase in the WO_3 filler loading resulted in an initial increase in the hardness of the composite, but a further increase in filler loading at 10 vol.% caused a reduction in hardness probably due to the undesirable agglomeration of the fillers. The initial increase in the hardness of the composites observed for both the nano-fillers and the micro-fillers may be attributed to their uniform dispersion within the epoxy matrix, together with their strong interaction with the epoxy chains to form good interfacial bonding.

6.3 Conclusions

The size effect of WO_3 particles on the X-ray transmission in nano-sized and micro-sized WO_3-epoxy composites has been investigated at various synchrotron radiation energies (i.e., 10–40 keV). The results presented in this work demonstrated that the size effect on X-ray attenuation was profoundly dependent on the energy of the synchrotron radiations. The particle size effect was more pronounced at lower synchrotron radiation energies (10–20 keV) since the X-ray transmission in nano-sized WO_3-epoxy composites was less than in their micro-sized counterparts. However, this size effect became insignificant at higher energies of 20–40 keV because the X-ray transmissions in both nano-sized and micro-sized WO_3-epoxy composites were very similar. The X-ray transmission results for the mammography unit sat between the results of 15–25 keV for XAS beam energies. Meanwhile, the X-ray transmissions in samples for X-ray tube voltages of 40–60 kV of the radiography unit sat between 25 and 40 keV. In addition, for composites with the same filler loading, but with increasing sample thickness, the size effect in X-ray transmission was most prominent for X-ray tube voltages of 25–35 kV but was negligible at 35–100 kV. As the filler loading of the WO_3 increased, the mechanical properties showed an initial optimum improvement, but a further increase in the filler loading caused these properties to deteriorate.

Acknowledgements The collection of X-ray absorption spectroscopy (XAS) data was funded by the Australian Synchrotron (AS123/XAS5341). We thank Dr. Bernt Johannessen of the Australian Synchrotron and our colleagues Dr. C. Ng and A/Prof. Z. Sun for assistance with XAS data collection. Also, we would like to thank Carolyn Madeley of Breast Assessment Centre, Royal Perth Hospital, Western Australia for giving us the opportunity to use the mammography unit.

References

1. Patra CR, Bhattacharya R, Mukhopadhyay D, Mukherjee P (2010) Fabrication of gold nanoparticles for targeted therapy in pancreatic cancer. Adv Drug Deliv Rev 62:346–361
2. Van Den Heuvel F, Locquet JP, Nuyts S (2010) Beam energy considerations for gold nanoparticle enhanced radiation treatment. Phys Med Biol 55:4509–4520

3. Wang T, Liu Z, Lu M, Wen B, Ouyang Q, Chen Y, Zhu C, Gao P, Li C, Cao M, Qi L (2013) Graphene-Fe3O4 nanohybrids: synthesis and excellent electromagnetic absorption properties. J Appl Phys 113:024314–024318
4. Hołyńska B (1969) Grain size effect in low energy gamma and X-ray scattering. Spectrochim Acta, Part B 24:85–93
5. Rad AG, Abbasi H, Afzali MH (2011) Gold nanoparticles: synthesising, characterizing and reviewing novel application in recent years. Phys Procedia 22:203–208
6. El Haber F, Froyer G (2008) Transparent polymers embedding nanoparticles for x-rays attenuation (Review). J Univ Chem Technol Metall 43:283–290
7. Jackson P, Periasamy S, Bansal V, Geso M (2011) Evaluation of the effects of gold nanoparticle shape and size on contrast enhancement in radiological imaging. Australas Phys Eng Sci Med 34:243–249
8. Huang X, El-Sayed MA (2010) Gold nanoparticles: Optical properties and implementations in cancer diagnosis and photothermal therapy. J Adv Res 1:13–28
9. Sahare PD, Ranju R, Numan S, Lochab SP (2007) K3Na(SO4)2: Eu nanoparticles for high dose of ionizing radiation. J Phys D Appl Phys 40:759
10. Popov A (2009) Sun protection using nanoparticles. SPIE Newsroom 24:1–2
11. Chen S-S, Chen H-C, Wang W-C, Lee C-Y, Lin IN, Guo J, Chang C-L (2013) Effects of high energy Au-ion irradiation on the microstructure of diamond films. J Appl Phys 113:113704–113710
12. Steinhart M (2004) Introduction to Nanotechnology. Angew Chem Int Ed 43:2196–2197
13. Botelho MZ, Künzel R, Okuno E, Levenhagen RS, Basegio T, Bergmann CP (2011) X-ray transmission through nanostructured and microstructured CuO materials. Appl Radiat Isot 69:527–530
14. Lablogic (2009) In: Lablogic Systems Limited (ed) Lablogic, Sheffield, United Kingdom
15. Daren S (2004) POLYMICRO Newsletter
16. Wardray. Wardray Premise Ltd, Surrey, United Kingdom, 2005–2011
17. Faccini M, Vaquero C, Amantia D (2012) Development of protective clothing against nanoparticle based on electrospun nanofibers. J Nanomater 2012:1–9
18. Künzel R, Okuno E (2012) Effects of the particle sizes and concentrations on the X-ray absorption by CuO compounds. Appl Radiat Isot 70:781–784
19. Noor Azman NZ, Siddiqui SA, Hart R, Low IM (2013) Effect of particle size, filler loadings and x-ray tube voltage on the transmitted x-ray transmission in tungsten oxide-epoxy composites. Appl Radiat Isot 71:62–67
20. Noor Azman NZ, Siddiqui SA, Low IM (2013) Characterisation of micro-sized and nano-sized tungsten oxide-epoxy composites for radiation shielding of diagnostic X-rays. Mater Sci Eng C 33:4952–4957
21. Park JJ (2013) Common spatial patterns based on generalized norms. Trans Electr Electron Mater 14:39–42
22. Moloney AC, Kausch HH, Kaiser T, Beer HR (1987) Review determining the strength and toughness of particulate filled epoxide resins. J Mater Sci 22:381–393